TAMPERE UNIVERSITY OF TECHNOLOGY

Joint Optimization of Communication and Traffic Efficiency in Vehicular Networks

Joint Optimization of Communication and Traffic Efficiency in Vehicular Networks

Long Zhao, *Member, IEEE*, Fangfei Wang, Kan Zheng, *Senior Member, IEEE*, and Taneli Riihonen, *Member, IEEE*

Abstract—Consider single-cell downlink vehicular networks, where a base station (BS) employing massive multiple-input multiple-output (MIMO) simultaneously transmits information to multiple vehicles on its covered road. Taking into account both the traffic and communication performance, the Flow rate of vehicles to the Power consumption of the BS Ratio (FPR) is defined as a comprehensive metric to represent the number of vehicles supported under limited transmit power. The objective of this paper is to maximize the FPR while guaranteeing the information rate requirements of the vehicles. We first derive the average power consumption of the BS with respect to vehicle density, based on which the FPR is established by using a flow rate function that quantifies the number of passed vehicles per time unit in terms of traffic density. Then, the optimal vehicle density is given in order to maximize the FPR. Simulation results indicate that the proposed scheme can significantly improve the power efficiency of the vehicular networks.

Index Terms—Vehicular networks, flow rate, power consumption.

I. Introduction

Vehicular networks are the typical applications of ultra-reliable low-latency communications (uRLLC) in fifth generation (5G) communications, and have gained much attention recently. Their objectives are to improve the transportation efficiency, traffic safety and quality of vehicle information services. To achieve these objectives, the literature has broadly investigated the architectures and key technologies of vehicular networks [1]–[5]. On the other hand, considering the traffic characteristics, such as flow rate, vehicle density and vehicle speed, etc., some communication metrics were also studied for vehicular networks [6]–[10].

Through analyzing the inter-arrival time and speed distributions of vehicles, the connection characteristics and routing performance were investigated for vehicular networks in [7]. Considering the vehicle density and vehicle speed, the packet delivery delay in vehicular ad hock networks was derived in [8]. Taking advantage of both vehicle density and channel state information (CSI), a joint macro and micro resource allocation

scheme was proposed in order to improve the latency based on software-defined vehicular networks in [9], [10]. However, the relationship between the traffic efficiency and communication efficiency is an open research area to our knowledge. The existing metrics can not describe the comprehensive performance of both the traffic and communication networks.

In the single-cell downlink communications, a base station (BS) employing massive multiple-input multiple-output (MIMO) simultaneously serves multiple vehicles on its covered road. In order to balance the traffic and communication efficiencies, this paper studies a new metric, i.e., the Flow rate of vehicles to the Power consumption of the BS Ratio (FPR). Guaranteeing the transmission rate requirements of all vehicles, the FPR is maximized in this paper. The transmission rate expression is given assuming a large number of antennas at the BS and the transmission rate constraints are transformed into the transmit power constraints. Then, the power consumption of the BS is analyzed and its average value is derived. Based on the obtained average power consumption, the tradeoff between the FPR and the vehicle density is established and, finally, the optimal FPR is then given by a nested bisection algorithm.

II. System Model and Problem Formulation

As illustrated in Fig. 1, an M-antenna BS using spatial multiplexing with bandwidth B transmits information to $K(L)$ single-antenna vehicles in multiple lanes. The BS is supposed to cover a road of length L from distance of H. To study the ultimate theoretical performance that can be achieved by the system, we assume the following traffic flow model without considering too many implementation-specific aspects [7]–[11].
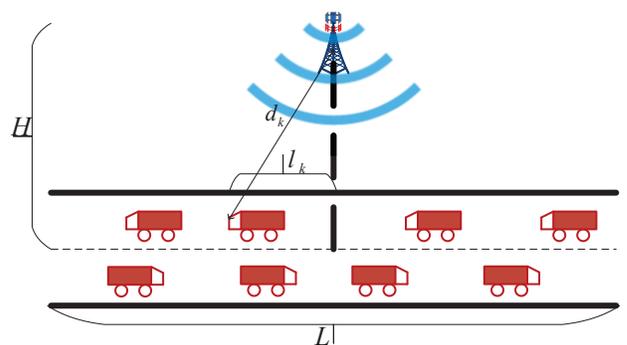

Fig. 1. Illustration of single-cell vehicular networks.

A. Traffic Flow Model

The number of vehicles on the road follows Poisson distribution:

$$P\{K(L)=k\} = \frac{(\rho L)^k}{k!}\mathrm{e}^{-\rho L}, k=1,2,\ldots, \quad (1)$$

where $\rho \geq 0$ denotes the average vehicle density [7]–[9].

The vehicle speeds can be assumed to be independent and identically distributed (i.i.d.), and the speed v_k of the kth vehicle follows a truncated normal distribution with the minimum speed v_{m} and maximum speed v_{M} [9], i.e.,

$$f(v_k) = \frac{\kappa(\bar{v},\sigma_v)}{\sqrt{2\pi}\sigma_v}\exp\left\{-\frac{(v_k-\bar{v})^2}{2\sigma_v^2}\right\}, v_k \in [v_{\mathrm{m}}, v_{\mathrm{M}}], \quad (2)$$

where the speed mean $\bar{v}$ is given by

$$\bar{v}(\rho) = v_{\mathrm{F}}\left(1-\frac{\rho}{\rho_{\mathrm{J}}}\right), \rho \in [0,\rho_{\mathrm{J}}], \quad (3)$$

with the free flow speed v_{F} and the jamming density ρ_{J}, the speed variance σ_v^2 is a constant, and the normalization factor is given by

$$\kappa(\bar{v},\sigma_v) = \left[\Phi\left(\frac{v_{\mathrm{M}}-\bar{v}}{\sigma_v}\right) - \Phi\left(\frac{v_{\mathrm{m}}-\bar{v}}{\sigma_v}\right)\right]^{-1}, \quad (4)$$

with $\Phi(y) = \int_{-\infty}^{y}\frac{1}{\sqrt{2\pi}}\exp\left(-x^2/2\right)\mathrm{d}x$.

The flow rate Q of the road is defined as the number of passed vehicles per second, which represents the traffic efficiency of the road. It can be calculated by the vehicle density ρ times the average vehicle speed $\bar{v}(\rho)$ [11], i.e.,

$$Q(\rho) = \rho\bar{v}(\rho) = v_{\mathrm{F}}\left(\rho - \frac{\rho^2}{\rho_{\mathrm{J}}}\right), \rho \in [0,\rho_{\mathrm{J}}]. \quad (5)$$

B. Communication Model

1) Channel Model: Denote $\mathbf{g}_k = \delta_k^{1/2}\mathbf{h}_k \in \mathbb{C}^{M\times 1}$ as the channel vector from the kth vehicle to the BS, where $\delta_k \in \mathbb{R}^+$ represents the large-scale fading and $\mathbf{h}_k = [h_{k,1}, h_{k,2}, \cdots, h_{k,M}]^{\mathrm{T}} \sim \mathbb{CN}(\mathbf{0}, \mathbf{I}_M)$ contains the fast fading coefficients. The large-scale fading $\delta_k = \phi d_k^{-\alpha}\xi_k$, where ϕ is a constant related to the antenna gain and carrier frequency, $d_k = \sqrt{H^2 + l_k^2}$ is the distance between the BS and the head of the kth vehicle (l_k denotes the distance between the head of the kth vehicle and the vertical line of the BS on the road, H represents the distance between the BS and the road, and the road width can be ignored compared with H), α denotes the path-loss exponent, and ξ_k refers to the shadow fading variable with $10\log_{10}\xi_k \sim \mathbb{N}(0,\sigma_{\mathrm{S}}^2)$. Considering the minimum mean square error (MMSE) channel estimation, we can assume that

$$\mathbf{h}_k = \sqrt{\theta}\hat{\mathbf{h}}_k + \sqrt{1-\theta}\mathbf{e}_k, \quad (6)$$

where the estimate $\hat{\mathbf{h}}_k \sim \mathbb{CN}(\mathbf{0},\mathbf{I}_M)$ is independent of the error $\mathbf{e}_k \sim \mathbb{CN}(\mathbf{0},\mathbf{I}_M)$ of $\mathbf{h}_k$, and $\theta \in [0,1]$ determines the estimation accuracy [12].

2) Transmission Model: In massive MIMO systems, matched-filter (MF) has been proved to be an asymptotically optimal precoder for information transmission [13], i.e., $\mathbf{w}_k = \hat{\mathbf{h}}_k^* / ||\hat{\mathbf{h}}_k^*||$, therefore is adopted in this paper. Assuming

that s_k with $|s_k| = 1$ and p_k/M are the modulation symbol and transmit power for the kth vehicle, the received signal of the kth vehicle is then given by

$$y_k = \mathbf{g}_k^{\mathrm{T}}\sum_{i=1}^{K(L)}\sqrt{\frac{p_i}{M}}\mathbf{w}_i s_i + n_k, \quad (7)$$

where the additive white Gaussian noise $n_k \sim \mathbb{CN}(0,\sigma^2)$.

According to the channel hardening effect, i.e., $\hat{\mathbf{h}}_k^{\mathrm{T}}\hat{\mathbf{h}}_k^*/M \to 1$, and asymptotic channel orthogonality, i.e., $\hat{\mathbf{h}}_k^{\mathrm{T}}\hat{\mathbf{h}}_i^*/M \to 0$ and $\mathbf{e}_k^{\mathrm{T}}\hat{\mathbf{h}}_i^*/M \to 0\,(i\neq k)$, for large M at the BS [13], the signal-to-interference-and-noise ratio (SINR) of the kth vehicle can be expressed as

$$\gamma_k = \frac{\frac{\theta p_k}{M}||\hat{\mathbf{h}}_k||^2}{\theta\sum_{i=1,\neq k}^{K(L)}\frac{p_i}{M}\frac{|\hat{\mathbf{h}}_k^{\mathrm{T}}\hat{\mathbf{h}}_i^*|^2}{||\hat{\mathbf{h}}_i^*||^2} + (1-\theta)\sum_{i=1}^{K(L)}\frac{p_i}{M}\frac{|\mathbf{e}_k^{\mathrm{T}}\hat{\mathbf{h}}_i^*|^2}{||\hat{\mathbf{h}}_i^*||^2} + \frac{\sigma^2}{\delta_k}}$$
$$\to \frac{p_k\theta\delta_k}{\sigma^2}, M \gg 1, \quad (8)$$

and the transmission rate can be approximated by

$$r_k(p_k) = B\log_2\left(1 + \frac{p_k\theta\delta_k}{\sigma^2}\right). \quad (9)$$

C. Power Consumption Model

Based on [14]–[16], the power consumption p_Σ of the BS contains in practice transmit power p_{T} for power amplifiers (PAs) and circuit power p_{C} for signal processing (such as coding, modulation, and RF links), i.e.,

$$p_\Sigma(\rho) = p_{\mathrm{T}}(\rho) + p_{\mathrm{C}}(\rho), \quad (10)$$

where

$$p_{\mathrm{T}}(\rho) = \frac{1}{\zeta M}\mathbb{E}\left[\sum_{k=1}^{K(L)}p_k\right], \text{ and} \quad (11)$$

$$p_{\mathrm{C}}(\rho) = \mathbb{E}\left[\sum_{i=0}^{1}(a_i + Mb_i)K^i(L) + c\sum_{k=1}^{K(L)}qv_k\right], \quad (12)$$

with ζ being the efficiency of PAs while $a_i\,(i=0,1)$, $b_i\,(i=0,1)$ and c being power consumption coefficients.

D. Problem Formulation

To guarantee traffic safety, the BS should timely transmit necessary position-related information to each vehicle, such as the surrounding vehicle information and map information. Therefore, the rate requirement of each vehicle is proportional to its speed, i.e., qv_k, where q [bit/m] denotes the required information amount of passing unit road length. Based on (9), the transmit power at the BS should satisfy $r_k(p_k) \geq qv_k$.

Guaranteeing the information rate requirements of all the vehicles, one objective of the vehicular networks is to maximize the supported flow rate $Q(\rho)$ and another objective is to minimize the power consumption of the BS $p_\Sigma(\rho)$. Therefore, the Flow rate of vehicles to the Power consumption of the BS Ratio (FPR) is defined for vehicular networks in this paper as

$$\eta(\rho) = \frac{Q(\rho)}{p_\Sigma(\rho)}, \quad (13)$$

and the considered optimization problem is formulated as

$$\max \ \eta(\rho) \tag{14}$$

$$\text{s.t. } 0 \le \rho \le \rho_{\text{J}}, \tag{15}$$

$$r_k(p_k) \ge qv_k, k = 1, 2, \ldots, K(L). \tag{16}$$

In the following sections, we first derive the average power consumption of the BS, then establish the relationship between the FPR η and vehicle density ρ, based on which the optimal vehicle density and FPR are given.

III. AVERAGE POWER CONSUMPTION

As shown by (9), $r_k(p_k)$ is a monotonically increasing function of p_k only and we can express p_k with respect to r_k. Therefore, the constraint (16) can be transformed into

$$p_k(\rho) \ge p_k^{\text{L}}(\rho) = \frac{\sigma^2}{\theta \delta_k}\left(2^{\frac{qv_k}{B}} - 1\right), \tag{17}$$

and we have the following results.

Proposition 1: To satisfy the minimum rate requirements qv_k $(k = 1, 2, \cdots, K(L))$ of all vehicles, the average power consumption of the BS is given by

$$p_{\Sigma}(\rho) = \chi_0\rho\left(e^{\chi_1+\chi_2\rho} - 1\right) + \chi_3\rho + \chi_4 + cqLQ(\rho), \tag{18}$$

where

$$\chi_0 = \frac{2\sigma^2}{\zeta M\theta\phi}\exp\left\{\frac{1}{2}\left(\sigma_{\text{S}}\frac{\ln 10}{10}\right)^2\right\}\int_0^{L/2}\left(H^2 + l_k^2\right)^{\alpha/2}\mathrm{d}l_k, \tag{19}$$

$$\chi_1 = \frac{q\ln 2}{2B}\left(\frac{q\sigma_v^2\ln 2}{B} - 2v_{\text{F}}\right), \chi_2 = \frac{qv_{\text{F}}\ln 2}{B\rho_{\text{J}}}, \tag{20}$$

$$\chi_3 = (a_1 + Mb_1)L, \text{ and } \chi_4 = a_0 + Mb_0. \tag{21}$$

Proof: We first analyze the average circuit power consumption, then the average transmit power consumption and finally the total power consumption of the BS.

Based on (1) and (2), we can obtain

$$\mathbb{E}[K(L)] = \rho L, \text{ and } \mathbb{E}[v_k] = \bar{v}. \tag{22}$$

Then, substituting (5) and (22) into (12) results in

$$p_{\text{C}}(\rho) = a_0 + Mb_0 + (a_1 + Mb_1)L\rho + cqLQ(\rho)$$
$$= \chi_4 + \chi_3\rho + cqLQ(\rho). \tag{23}$$

Substituting (17) and $\delta_k = \phi d_k^{-\alpha}\xi_k$ into (11), the power consumption of the PAs can be rewritten as

$$p_{\text{T}}(\rho) = \frac{\sigma^2}{\zeta M\theta\phi}\mathbb{E}\left\{\sum_{k=1}^{K(L)}\mathbb{E}\left[d_k^{-\alpha}\right]\mathbb{E}\left[\xi_k^{-1}\right]\left(\mathbb{E}\left[2^{\frac{qv_k}{B}}\right] - 1\right)\right\}. \tag{24}$$

According to the distribution of shadow fading, i.e.,

$$f_{\xi_k}(\xi) = \frac{\kappa}{\xi}\frac{1}{\sqrt{2\pi}\sigma_{\text{F}}}\exp\left\{-\frac{(\kappa\ln\xi)^2}{2\sigma_{\text{F}}^2}\right\}, \kappa = \frac{10}{\ln 10}, \tag{25}$$

we can obtain $\mathbb{E}\left[\xi_k^{-1}\right] = \exp\left[\frac{1}{2}\left(\frac{\sigma_{\text{S}}\ln 10}{10}\right)^2\right]$. According to the

vehicle speed distribution in (2), we have

$$\mathbb{E}\left[2^{\frac{qv_k}{B}}\right] = \frac{\kappa(\bar{v}, \sigma_v)\exp\left\{\frac{q\ln 2}{2B}\left(\frac{q\sigma_v^2\ln 2}{B} - 2\bar{v}\right)\right\}}{\kappa\left(\bar{v} - \frac{q\sigma_v^2\ln 2}{B}, \sigma_v\right)}. \tag{26}$$

When $\bar{v} \gg q\sigma_v^2\ln 2/B$, substituting (3) into (26) gives rise to

$$\mathbb{E}\left[2^{\frac{q}{B}v_k}\right] \approx \exp\left\{\frac{q\ln 2}{2B}\left(\frac{q\sigma_v^2\ln 2}{B} - 2v_{\text{F}}\right) + \frac{qv_{\text{F}}\ln 2}{B\rho_{\text{J}}}\rho\right\}$$
$$= \exp\{\chi_1 + \chi_2\rho\}. \tag{27}$$

Based on (1), the vehicles' positions are i.i.d. on the road, i.e, $f(l_k) = 1/L$. Then, we can obtain

$$\mathbb{E}\left\{\sum_{k=1}^{K(L)}\mathbb{E}\left[d_k^{-\alpha}\right]\right\} = \mathbb{E}\left\{\sum_{k=1}^{K(L)}\mathbb{E}\left[\left(H^2 + l_k^2\right)^{\alpha/2}\right]\right\}$$

$$= \sum_{K(L)=1}^{+\infty}K(L)\int_0^{L/2}\left(H^2 + l_k^2\right)^{\alpha/2}\frac{2}{L}\mathrm{d}l_k\frac{(\rho L)^{K(L)}}{K(L)!}e^{-\rho L}$$

$$= 2\rho e^{-\rho L}\sum_{K(L)=1}^{+\infty}\frac{(\rho L)^{K(L)-1}}{[K(L)-1]!}\int_0^{L/2}\left(H^2 + l_k^2\right)^{\alpha/2}\mathrm{d}l_k$$

$$= 2\rho\int_0^{L/2}\left(H^2 + l_k^2\right)^{\alpha/2}\mathrm{d}l_k. \tag{28}$$

Hence, the total transmit power of the PAs can be written as

$$p_{\text{T}}(\rho) = \chi_0\rho\left(e^{\chi_1+\chi_2\rho} - 1\right). \tag{29}$$

Finally, substituting (23) and (29) into (10) leads to (18). ∎

IV. TRADEOFF BETWEEN FPR AND VEHICLE DENSITY

Because the FPR is a decreasing function of power consumption, $p_k(\rho) = p_k^{\text{L}}(\rho)$ will maximize the FPR. Then, substituting (5) and (18) into (13), we can obtain the tradeoff between the FPR η and the vehicle density ρ, given by

$$\eta(\rho) = \left[\frac{\chi_0\rho(e^{\chi_1+\chi_2\rho} - 1) + \chi_3\rho + \chi_4}{Q(\rho)} + cqL\right]^{-1}. \tag{30}$$

Proposition 2: To achieve the optimal FPR η^* in the considered vehicular networks, the vehicle density should satisfy

$$\rho = \min\{\max\{\tilde{\rho}(\eta^*), 0\}, \rho_{\text{J}}\}, \tag{31}$$

where $\tilde{\rho}(\eta^*)$ implicitly satisfies

$$\chi_0(1+\chi_2\tilde{\rho})e^{\chi_1+\chi_2\tilde{\rho}} + (\eta^{-1}-cqL)v_{\text{F}}(2\tilde{\rho}/\rho_{\text{J}}-1) = \chi_0-\chi_3, \tag{32}$$

and can be explicitly solved with bi-section search. Likewise, the optimal FPR η^* can also be obtained by bi-section search.

Proof: As (16) has become $p_k(\rho) = p_k^{\text{L}}(\rho)$ to maximize the FPR and was used to calculate the power consumption of PAs, the problem in (14)–(16) is transformed into

$$\min\left\{\eta^{-1}(\rho)\right\} \text{ s.t. } 0 \le \rho \le \rho_{\text{J}}. \tag{33}$$

Defining $f(\rho) = \chi_0\rho(e^{\chi_1+\chi_2\rho} - 1) + \chi_3\rho + \chi_4$, we have $\mathrm{d}^2f(\rho)/\mathrm{d}\rho^2 = (2 + \chi_2\rho)\chi_0\chi_2 e^{\chi_1+\chi_2\rho} > 0$ so that $f(\rho)$ is convex, while $Q(\rho)$ is a concave function of ρ. Based on [17], if the objective has a convex numerator and a concave

denominator, the problem in (33) is equivalent to

$$\min\ g\left(\rho;\eta\right)=f\left(\rho\right)-\left(\eta^{-1}-cqL\right)Q\left(\rho\right)\ \text{s.t.}\ 0\leq\rho\leq\rho_{\text{J}},\ (34)$$

and the optimal FPR η^* satisfies

$$g\left(\rho;\eta\right)\begin{cases} > 0, & \eta > \eta^*, \\ = 0, & \eta = \eta^*, \\ < 0, & \eta < \eta^*. \end{cases} \tag{35}$$

Given η, the Lagrange function of (34) can be expressed as

$$\mathcal{L}\left(\rho;\lambda,\mu\right)=g\left(\rho;\eta\right)+\lambda\left(\rho-\rho_{\text{J}}\right)-\mu\rho, \tag{36}$$

and $\partial\mathcal{L}\left(\rho;\lambda,\mu\right)/\partial\rho = \chi_0\left(1+\chi_2\rho\right)\mathrm{e}^{\chi_1+\chi_2\rho} - \chi_0 + \chi_3 + \lambda-\mu-\left(\eta^{-1}-cqL\right)v_{\text{F}}\left(1-2\rho/\rho_{\text{J}}\right)$. According to the Karush-Kuhn-Tucker (KKT) conditions [18], we can obtain

$$\partial\mathcal{L}\left(\rho;\lambda,\mu\right)/\partial\rho = 0, \tag{37}$$
$$\lambda\left(\rho-\rho_{\text{J}}\right)=0,\ \mu\rho=0. \tag{38}$$

When $0 < \rho < 1$, i.e., $\lambda = \mu = 0$, we define

$$h\left(\rho\right)=\chi_0\left(1+\chi_2\rho\right)\mathrm{e}^{\chi_1+\chi_2\rho} - \left(\eta^{-1}-cqL\right)v_{\text{F}}\left(1-2\rho/\rho_{\text{J}}\right) - \chi_0 + \chi_3, \tag{39}$$

and the first-order derivative of $h\left(\rho\right)$ is given by $\mathrm{d}h\left(\rho\right)/\mathrm{d}\rho = \chi_0\chi_2\left(2+\chi_2\rho\right)\mathrm{e}^{\chi_1+\chi_2\rho} + 2\left(\eta^{-1}-cqL\right)v_{\text{F}}/\rho_{\text{J}} > 0$. Therefore, $h\left(\rho\right)$ is a monotonically increasing function with respect to the vehicle density ρ and the bisection search method can be employed to solve (37) with $\lambda = 0$ and $\mu = 0$, i.e., (32) [18]. Further, taking into account (38) with $\lambda \neq 0$ and $\mu \neq 0$, the optimal vehicle density should meet (31). ∎

Based on *Proposition 2* and (35), the optimal FPR η^* can be obtained by *Algorithm 1*, which contains two nested loops. The outer loop finds the optimal FPR and the inner loop calculates the optimal vehicle density for a given FPR value. Moreover, the initial values of both η and ρ should constitute ranges such that $\rho^* \in [\rho_{\text{L}}, \rho_{\text{U}}]$ and $\eta^* \in [\eta_{\text{L}}, \eta_{\text{U}}]$. According to (5), we can set $\rho_{\text{L}} = 0$ and $\rho_{\text{U}} = \rho_{\text{J}}$. Based on (30), $\eta \leq 1/\left(cqL\right)$ and therefore we set $\eta_{\text{U}} = 1/\left(cqL\right)$. On the other hand, $\eta^{-1}(\rho)$ is a quasi-convex function, any $\rho \in [0, \rho_{\text{J}}]$ can satisfy $\eta_{\text{L}} = \eta\left(\rho\right) \leq \eta^*$ and we set $\eta_{\text{L}} = \eta(\rho_{\text{J}}/2)$.

Algorithm 1 : Nested Bisection Algorithm for the Optimal FPR

Initialization: $\eta_{\text{U}}= 1/\left(cqL\right)$, $\eta_{\text{L}}=\eta\left(\rho_{\text{J}}/2\right)$, error tolerance $\varepsilon_{\eta}>0$.
  1: Let $\eta = \left(\eta_{\text{L}} + \eta_{\text{U}}\right)/2$.
  2: Initialize $\rho_{\text{L}} = 0$, $\rho_{\text{U}} = \rho_{\text{J}}$, and error tolerance $\varepsilon_{\rho} > 0$.
    2.1: Let $\rho = \left(\rho_{\text{L}} + \rho_{\text{U}}\right)/2$;
    2.2: Calculate $h\left(\rho\right)$ based on (39);
    2.3: If $h\left(\rho\right) > 0$, let $\rho_{\text{U}} = \rho$; Else $\rho_{\text{L}} = \rho$;
    2.4: If $|h\left(\rho\right)| < \varepsilon_{\rho}$, let $\rho = \left(\rho_{\text{L}} + \rho_{\text{U}}\right)/2$; Else go to **2.1**.
  3: Calculate $\eta\left(\rho\right)$ and $g\left(\eta,\rho\right)$ by (30) and (34), respectively.
  4: If $g\left(\eta,\rho\right) > 0$, then $\eta_{\text{U}} = \eta$; Else $\eta_{\text{L}} = \eta$.
  5: If $\eta_{\text{U}}-\eta_{\text{L}} < \varepsilon_{\eta}$, let $\eta^*= \left(\eta_{\text{L}}+\eta_{\text{U}}\right)/2$; Else go to **1**.
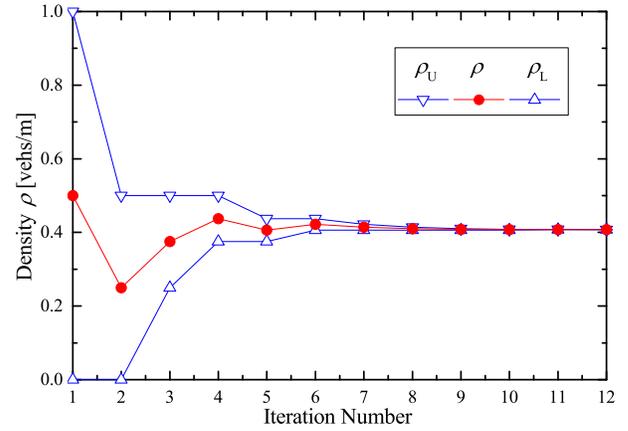

Fig. 2. Convergence of Algorithm 1 ($q = 2.5 \times 10^5$ bit/m).

V. NUMERICAL RESULTS AND ANALYSIS

A. Parameter Setup

In the simulation, the default parameters are given as follows. The number of antennas at the BS is $M = 10000$, the system bandwidth is $B = 200$ kHz, and the information requirement of each vehicle per meter is $q = 2.5 \times 10^5$ bit/m [7], [9], [13]. The distance between the BS and the road is $H = 250$ m, the road length covered by the BS is $L = 2H/\sqrt{3}$, the constant $\phi = 10^{-3}$, the standard variance of shadow fading $\sigma_{\text{S}} = 8$ dB, the path-loss exponent $\alpha = 4$, and the noise power $\sigma^2 = BN$ with the noise power spectrum density $N = -174$ dBm/Hz [9], [19]–[21]. The free flow speed $v_{\text{F}} = 35$ m/s, the minimum vehicle speed $v_{\text{m}} = 5$ m/s, the maximum vehicle speed $v_{\text{M}} = v_{\text{F}}$, the speed standard variance $\sigma_v = 10$ m/s, and the jamming density $\rho_{\text{J}} = 1$ vehs/m [7]–[10]. The power efficiency of PAs is $\eta = 0.28$, the power consumption coefficients are $[a_0, a_1] = [20, 0.1]$ W, $[b_0, b_1] = \left[1, 2.6 \times 10^{-8}\right]$ W, and $c = 1.15 \times 10^{-9}$ W/bit [14]–[16]. "PCSI" and "ECSI" are the abbreviations of "perfect CSI" and "estimated CSI" in the following figures, respectively.

B. FPR Results

With $q = 2.5 \times 10^5$ bit/m, Fig. 2 plots the vehicle density ρ versus the number of inner iterations for the first outer iteration of *Algorithm 1* under the perfect CSI case, where ρ_{L}, ρ_{U} and ρ represent the lower bound, upper bound and the obtained vehicle density of each inner iteration. With the increasing number of iterations, the upper bound decreases and the lower bound increases, and they rapidly converge to a constant, which verify the convergence of the inner iteration of *Algorithm 1* under the perfect CSI case. Moreover, the convergence behavior of the outer iteration and the estimated CSI case are similar to that of the inner iteration.

The FPR versus the flow rate is illustrated in Fig. 3 with $q = 2.5 \times 10^5$ bit/m, $\varepsilon_{\eta} = 10^{-6}$ and $\varepsilon_{\rho} = 10^{-10}$. Moreover, the optimal FPR points obtained by *Algorithm 1* and the optimal flow rate points obtained by traditional setup, i.e., $\rho = \rho_{\text{J}}/2$ [11], are also given in Fig. 3. With the increasing vehicle density ρ, both the FPR and flow rate first increase and then decrease. The optimal FPR points locate on the
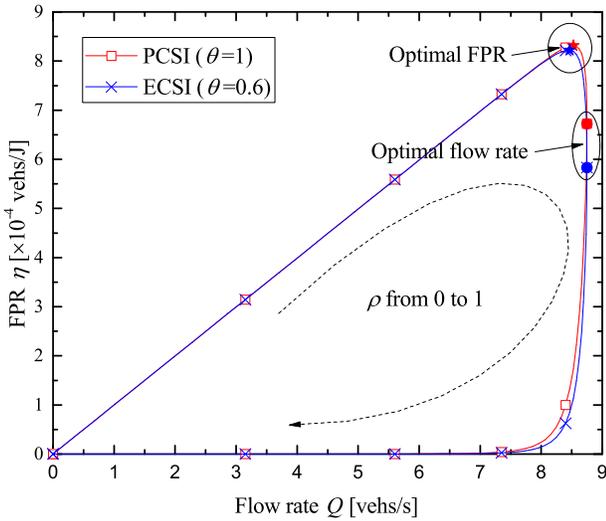
Fig. 3. FPR versus flow rate ($q = 2.5 \times 10^5$ bit/m, $\varepsilon_\eta = 10^{-6}$ and $\varepsilon_\rho = 10^{-10}$).
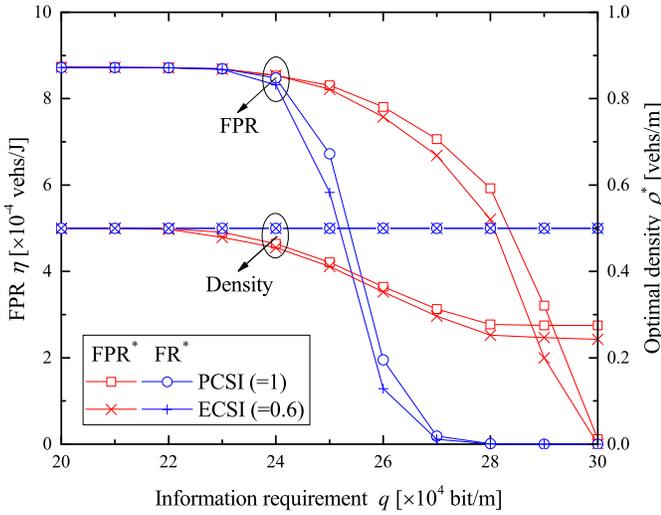

Fig. 4. Optimal FPR versus information requirement ($\varepsilon_\eta = 10^{-6}$ and $\varepsilon_\rho = 10^{-10}$).

tops of the tradeoff curves and outperform the FPR points corresponding to the optimal flow rates, which validates the optimality of *Algorithm 1*. Moreover, the tradeoff under perfect CSI outperforms that under estimated CSI due to the more accurate CSI. With $\varepsilon_\eta = 10^{-6}$ and $\varepsilon_\rho = 10^{-10}$, the optimal FPR (labeled by FPR* in Fig. 4) and the FPR (labeled by FR* in Fig. 4) under the optimal flow rate (i.e., traditional setup) as well as their corresponding vehicle densities versus the information requirement are shown in Fig. 4. With the increasing information requirement, both the optimal FPR and vehicle density decrease because more transmit power is consumed by PAs. The optimal FPR outperforms the FPR under the optimal flow rate and the FPR under perfect CSI performs better than that under estimated CSI.

VI. CONCLUSION

To improve the traffic efficiency and simultaneously reduce the communication cost of vehicular networks, the objective of this paper is to find the maximal FPR while satisfying the rate requirements of vehicles. Based on the derived power consumption of the BS and the flow rate function, the tradeoff between the FPR and vehicle density is formulated. Then, the optimal FPR is obtained by a proposed bisection search algorithm. Results indicate that the proposed scheme can balance the power consumption and the traffic efficiency.

REFERENCES

[1] K. Zheng, L. Hou, H. Meng, Q. Zheng, N. Lu, and L. Lei, "Soft-defined heterogeneous vehicular network: Architecture and challenges," *IEEE Netw.*, vol. 30, no. 4, pp. 72-80, Jul. 2016.

[2] S. Correia, A. Boukerche, and R. I. Meneguette, "An architecture for hierarchical software-defined vehicular networks," *IEEE Commun. Mag.*, vol. 55, no. 7, pp. 80-86, Jul. 2017.

[3] W. Shi, H. Zhou, J. Li, W. Xu, N. Zhang, and X. Shen, "Drone assisted vehicular networks: Architecture, challenges and opportunities," *IEEE Netw.*, vol. 32, no. 3, pp. 130-137, May/Jun. 2018.

[4] Y. Sun, L. Xu, Y. Tang, and W. Zhuang, "Traffic offloading for online video service in vehicular networks: A cooperative approach," *IEEE Trans. Veh. Technol.*, vol. 67, no. 8, pp. 7630-7642, Aug. 2018.

[5] K. Zheng, H. Meng, P. Chatzimisios, L. Lei, and X. Shen, "An SMDP-based resource allocation in vehicular cloud computing systems," *IEEE Trans. Ind. Electron.*, vol. 62, no. 12, pp. 7920-7928, Dec. 2015.

[6] J. Wang, Y. Huang, Z. Feng, C. Jiang, H. Zhang, and V. C. M. Leung, "Reliability traffic density estimation in vehicular network," *IEEE Trans. Veh. Technol.*, vol. 67, no. 7, pp. 6424-6437, Jul. 2018.

[7] N. Wisitpongphan, F. Bai, P. Mudalige, V. Sadekar, and O. Tonguz, "Routing in sparse vehicular Ad Hoc wireless networks," *IEEE J. Sel. Areas Commun.*, vol. 25, no. 8, pp. 1538-1556, Oct. 2007.

[8] A. Abdrabou and W. Zhuang, "Probabilistic delay control and road side unit placement for vehicular ad hoc networks with disrupted connectivity," *IEEE J. Sel. Area Commun.*, vol. 29, no. 1, pp. 129-139, Jan. 2011.

[9] Q. Zheng, K. Zheng, H. Zhang, and V. C. M. Leung, "Delay-optimal virtualized radio resource scheduling in software-defined vehicular networks via stochastic learning," *IEEE Trans. Veh. Technol.*, vol. 65, no. 10, pp. 7857-7867, Oct. 2016.

[10] M. J. Khabbaz, W. F. Fawaz, and C. M. Assi, "A simple free-flow traffic model for vehicular intermittently connected networks," *IEEE Trans. Intell. Transp. Syst.*, vol. 13, no. 3, pp. 1312-1326, Sep. 2012.

[11] D. Ni, *Traffic flow theory: Characteristics, experimental methods, and numerical techniques*. Butterworth-Heinemann: Oxford, Oct. 2015.

[12] W. Xu, J. Liu, S. Jin, and X. Dong, "Spectral and energy efficiency of multi-pair massive MIMO relay network with hybrid processing," *IEEE Trans. Commun.*, vol. 65, no. 9, pp. 3794-3808, Sep. 2017.

[13] E. Björnson, E. G. Larsson, and T. L. Marzetta, "Massive MIMO: Ten myths and one critical question," *IEEE Commun. Mag.*, vol. 54, no. 2, pp. 114-123, Feb. 2016.

[14] E. Bjornson, L. Sanguinetti, J. Hoydis, and M. Debbah, "Optimal design of energy-efficient multi-user MIMO systems: Is massive MIMO the answer?," *IEEE Trans. Wireless Commun.*, vol. 14, no. 6, pp. 3059-3075, Jun. 2015.

[15] L. Zhao and X. Wang, "Round-trip energy efficiency of wireless energy powered massive MIMO system with latency constraint," *IEEE Commun. Lett.*, vol. 21, no. 1, pp. 12-15, Jan. 2017.

[16] Z. Xu, C. Yang, G. Y. Li, S. Zhang, Y. Chen, and S. Xu, "Energy-efficient configuration of spatial and frequency resources in MIMO-OFDMA systems," *IEEE Trans. Commun.*, vol. 61, no. 2, pp. 564-575, Feb. 2013.

[17] K. Shen and W. Yu, "Fractional programming for communication systems-part I: Power control and beamforming," *IEEE Trans. Signal Process.*, vol. 66, no. 10, pp. 2616-2630, May 2018.

[18] S. Boyd and L. Vandenberghe, *Convex Optimization*. Cambridge University Press: New York, 2004.

[19] L. Liang, H. Peng, G. Y. Li, and X. Shen, "Vehicular communications: A physical layer perspective," *IEEE Trans. Veh. Technol.*, vol. 66, no. 12, pp. 10647-10659, Dec. 2017.

[20] L. Zhao, X. Wang, and K. Zheng, "Downlink hybrid information and energy transfer with massive MIMO," *IEEE Trans. Wireless Commun.*, vol. 15, no. 2, pp. 1309-1322, Feb. 2016.

[21] M. Sadeghi, E. Björnson, E. G. Larsson, C. Yuen, and T. L. Marzetta, "Max-min fair transmit precoding for multi-group multicasting in massive MIMO," *IEEE Trans. Wireless Commun.*, vol. 17, no. 2, pp. 1358-1372, Feb. 2018.